Supporting Information for

N, P, and S co-doped 3D Porous Carbon Architectured Cathode for High-performance Zn-ion Hybrid Capacitor

Kezheng Shang[1,2], Yangjie Liu[1], Pingwei Cai[1,2], Kangkang Li*[,3], Zhenhai Wen*[1,2]

[1] *CAS Key Laboratory of Design and Assembly of Functional Nanostructures, Fujian Provincial Key Laboratory of Nanomaterials, Fujian Institute of Research on the Structure of Matter, Chinese Academy of Sciences, Fuzhou 350002, P. R. China.*

[2] *University of Chinese Academy of Sciences, Beijing 100049, P. R. China.*

3 CSIRO Energy, 10 Murry Dwyer Circuit, Mayfield West, NSW 2304, Australia

* Corresponding authors
E-mail: wen@fjirsm.ac.cn, kangkang.li@csiro.au

Experimental Section

Materials: Phosphonitrilic chloride trimer ($N_3P_3Cl_6$, 98%), 4,4'-Sulfonyldiphenol ($C_{12}H_{10}O_4S$, 98%), Tetraethyl orthosilicate ($C_8H_{20}O_4Si$, 98%), Triethylamine ($C_6H_{15}N$, 99%), Ammonium hydroxide (NH_3(aq), 25%-28%), Methanol (CH_4O, 99.5%), Ethanol absolute (C_2H_6O, 99.7%). All chemicals were used as received without further purification.

Synthesis of SiO_2 spheres: Typically, 10 ml deionized water and 3 ml $NH_3 \cdot H_2O$ were added in 75 ml ethanol absolute under stirring 10 min to get homogeneous solution. Afterward, 6 ml tetraethyl orthosilicate was added in the solution and reacted at 35℃ for 3 hours. The synthesized product was obtained by centrifugation, and then washed with deionized water and ethanol three times successively, and dried under vacuum at 60℃ to directly obtain white SiO_2 spheres.

Synthesis of HPCS: 400 mg SiO_2 spheres was dispersed in 80 ml methanol under vigorously stirring for 30 min, denoted as solution A. 0.56 g phosphonitrilic chloride trimer and 1.26 g 4,4'-sulfonyldiphenol were dispersed in 40 ml methanol, denoted as solution B. Then, the solution B was slowly added dropwise to the solution A with a separating funnel. After 10 min, 1 ml triethylamine was added in the above solution and the solution was stirred for another 6 hours. After that, the synthesized product was obtained by centrifugation, and washed with ethanol three times, and dried under vacuum at 60 ℃ overnight. The sample was calcined at 800 ℃, 900 ℃ and 1000 ℃ under the Ar atmosphere with a heating rate of 2 ℃ min^{-1}, and then etched by NaOH aqueous solution. Finally, the black sample was washed several times with deionized water, and dried at 60 ℃ in vacuum to obtain the HPCS.

Synthesis of the contrast sample PCS-900 (Porous carbon spheres): 0.56 g phosphonitrilic chloride trimer and 1.26 g 4,4'-sulfonyldiphenol were dispersed in 40 ml methanol. After 10 min, 1 ml triethylamine was added in the above solution and it reacted for 2 hours in an ultrasonic bath (150 W), the centrifugation as described above. The sample was calcined at 900 ℃ under the Ar atmosphere with a heating rate of 2 ℃ min^{-1}.

Electrochemical measurements

For the Zn-ion hybrid supercapacitor, the slurry was first prepared by dispersing the active materials, polyvinylidene difluoride (PVDF) and Super P in N-methyl-2-pyrrolidone (NMP) with a weight ratio of 8:1:1. The slurry was cast on the titanium foil (diameter = 1.2 cm) and then dried in a vacuum at 70 ℃ for 24 hours (the active material loading of each electrode is 0.8-0.9 mg). The CR2032 coin-type cell was assembled with Zn metal foil as the negative electrode, Whatman glass fibers as the separator, and 3M $ZnSO_4$ as the electrolyte. For a soft-pack ZIHCs device, this ZIHCs was sealed up in aluminum plastic films with a heat-sealing machine by employing the fabricated HPCS/Ti electrode (2*2 cm^2, the load mass of active materials ≈ 0.8 mg cm^{-2}) as the cathode, Zn foil (2*2 cm^2) as the anode, Whatman glass fibers as the separator and 3M $ZnSO_4$ as the electrolyte. In the three-electrode electrochemical measurements, Pt electrode and Calomel electrode were used as counter electrode and reference electrode. The Cyclic voltammetry (CV) curves and electrochemical impedance spectroscopy (EIS) were performed on a CHI660E electrochemical workstation. Electrochemical impedance spectroscopy was collected in a frequency range from 0.01 Hz to 100 kHz. In the galvanostatic charge/discharge test, the ZIHCs was measured in the voltage range from 0.1 V to 1.7 V in a LAND multichannel battery test system (Wuhan Kingnuo Electronic Co., China).

Material characterization

The morphology and microstructure of the were observed through field emission scanning electron microscopy (FESEM, Hitachi SU-8020), and transmission electron microscopy (TEM, Talos-F200X). The X-ray diffraction was tested by Miniflex 600 powder X-ray diffractometer (Cu-Kα radiation, λ =1.54178 Å) and Raman spectra was measured using a LabRam HR800 spectrometer. Nitrogen sorption isotherm and the pore size distribution were conducted on the Intelligent Gravimetric Sorption Analyser (IGA100B). And X-ray photoelectron spectroscopy (XPS) was measured on ESCALAB 250Xi (Thermo Fisher). Thermogravimetric analysis (TGA, NETZSCH STA449F3) was employed to characterize the mass percentage of samples.

Calculation

The specific capacity (C_m, mAh g^{-1}) for ZIHCs was calculated from the galvanometric charge-discharge curves using the following equations:

$$C_m = 2I \int V\, dt/3.6Vm \quad \text{(S1)}$$

where I (A), $\int V dt$ (Vs), V (V) and m (g) represent the discharge current (A), the integral area under charge/discharge curve, the voltage after ohmic drop, and the mass of active material in cathode, respectively.

The specific gravimetric capacitance (C, F g^{-1}) for ZIHCs was calculated from the galvanometric charge-discharge curves using the following equations:

$$C = It/mV \quad \text{(S2)}$$

where t (s) is the discharge time.

Energy density and power density for the ZIHCs device were calculated based on the mass of active material of cathode using the following equations:

$$E = 1/7.2\, CV^2 \quad \text{(S3)}$$

$$P = 3600E/t \quad \text{(S4)}$$

Where C (F g^{-1}) is the specific gravimetric capacitance calculated above, E (Wh kg^{-1}) is the energy density, P (W kg^{-1}) is the power density, t (s) is the discharge time.

Calculation of the b Value and Capacitive Contribution:

The measured current of CV curves could be separated into two types of charge storage for ZIHCs electrode materials, surface capacitive dominated processes and diffusion-controlled processes. Generally, the charge storage kinetics mechanism can be investigated by the power-law relationship between the measured current density (i) and the sweep rate (v) based on the following formulas:

$$i = av^b \tag{S5}$$

where a and b are variables, and the b value of 0.5 denotes a totally faradaic intercalation process and the b value of 1 indicates an ideally capacitive contribution process.

Quantitatively, the mixed behaviors can be further distinguished by separating the current response (i) at a specific potential (V) according to the following equations:

$$i(\mathrm{V}) = i_{cap} + i_{diff} = k_1 v + k_2 v^{1/2} \tag{S6}$$

Equation (S6) can be converted to Equation (S7):

$$i(\mathrm{V})/v^{1/2} = k_1 v^{1/2} + k_2 \tag{S7}$$

where both k_1 and k_2 are constant values, $k_1 v$ and $k_2 v^{1/2}$ represent the contribution from surface capacitive behavior and contribution of diffusion-dominated reaction, respectively.

Supporting Figure

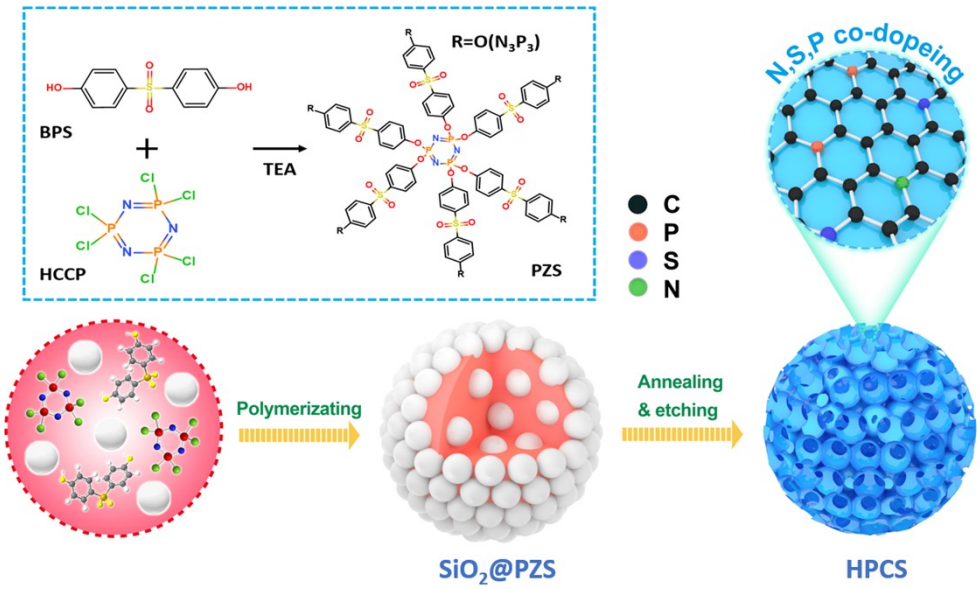

Figure S1. Schematic diagram of the synthetic process of HPCS.

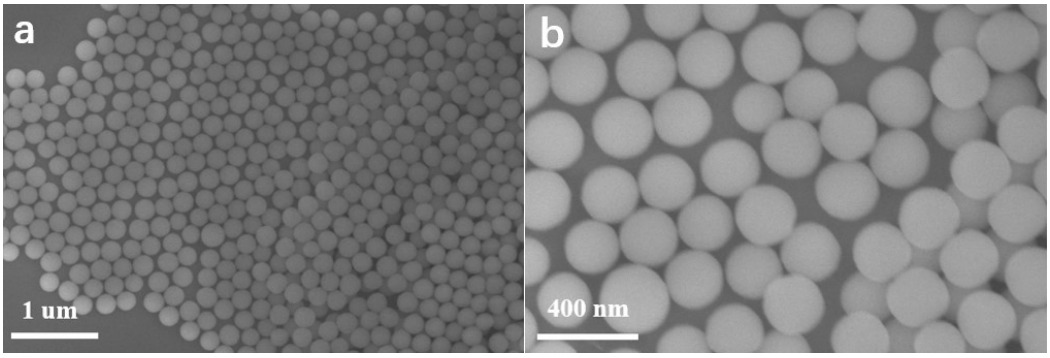

Figure S2. SEM images of SiO_2 spheres.

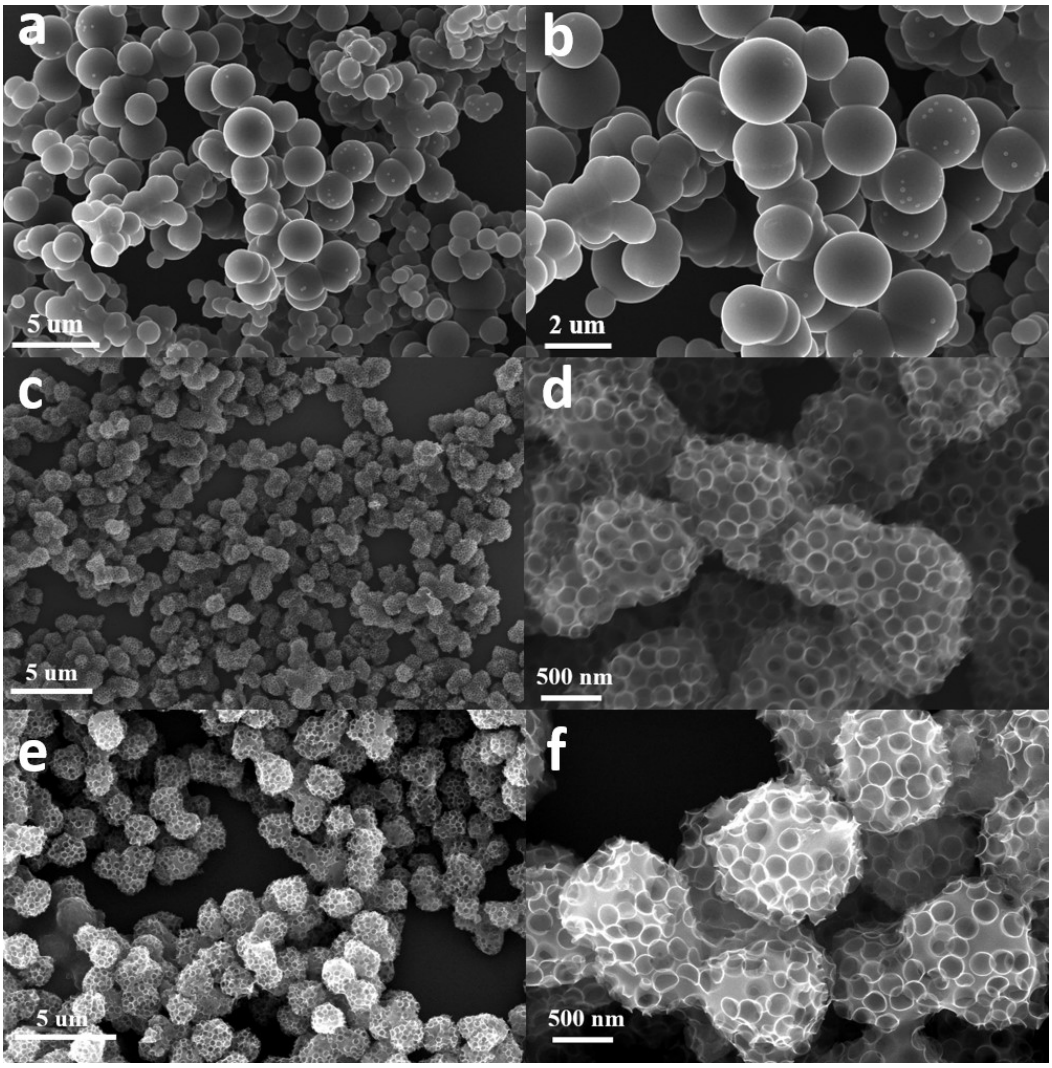

Figure S3. SEM images of (a-b) the contrast sample PCS-900, (c-d) the HPCS-800 and (e-f) the HPCS-1000.

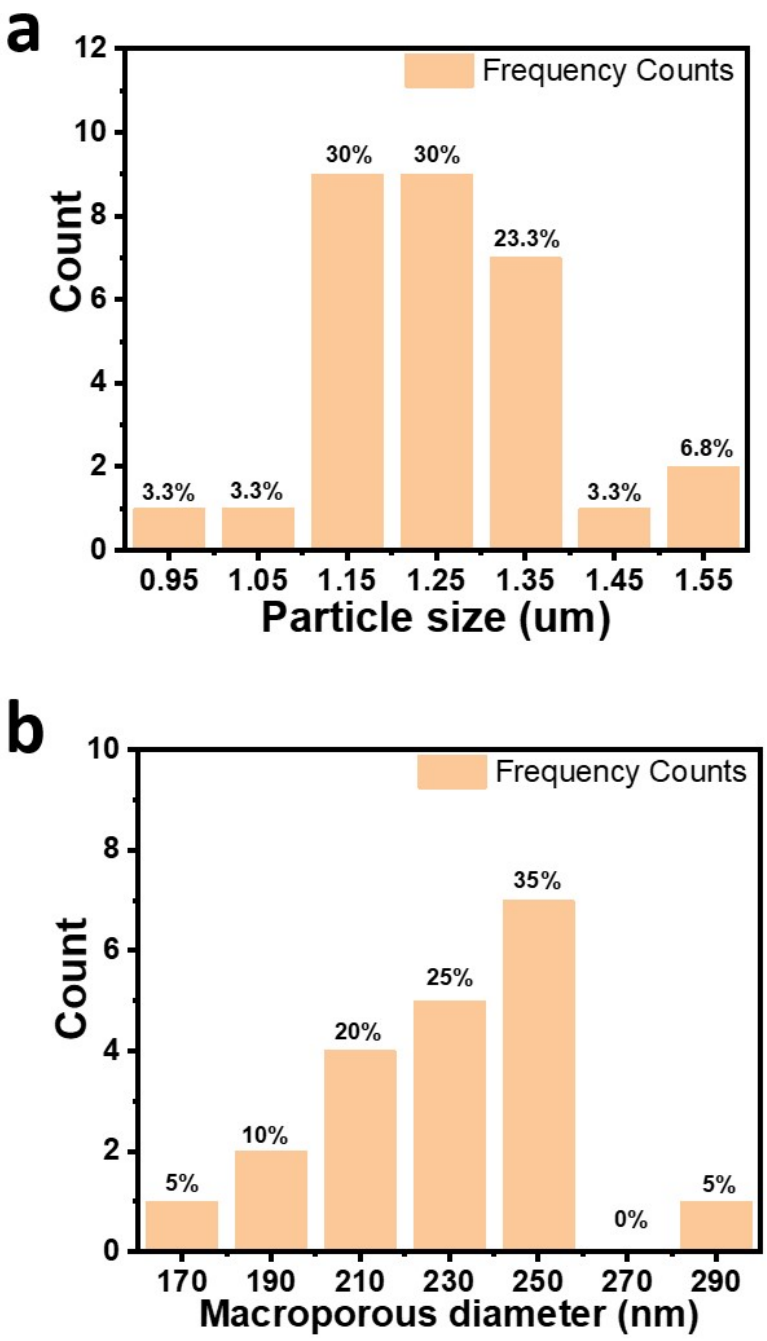

Figure S4. The HPCS-900 of (a) particle size distribution and (b) macroporous size distribution.

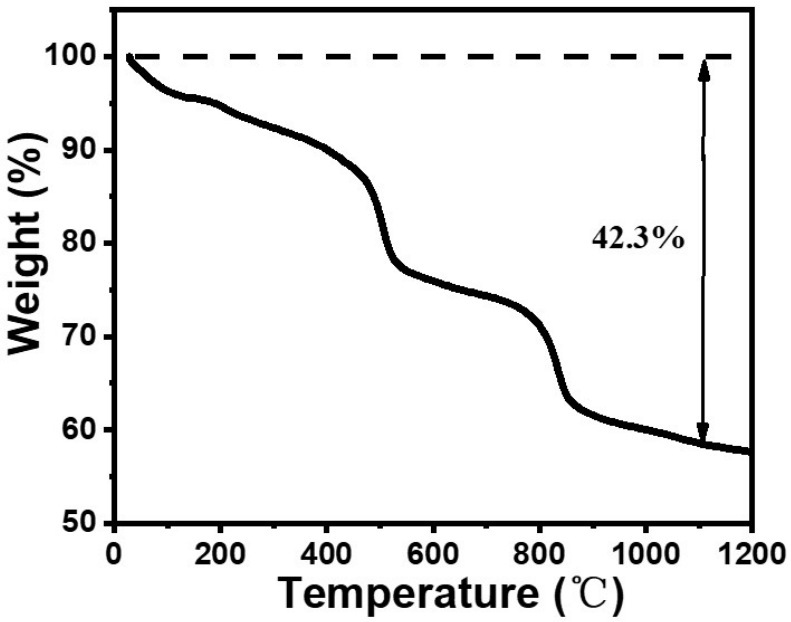

Figure S5. TG curves of the polymer precursors in Ar atmosphere.

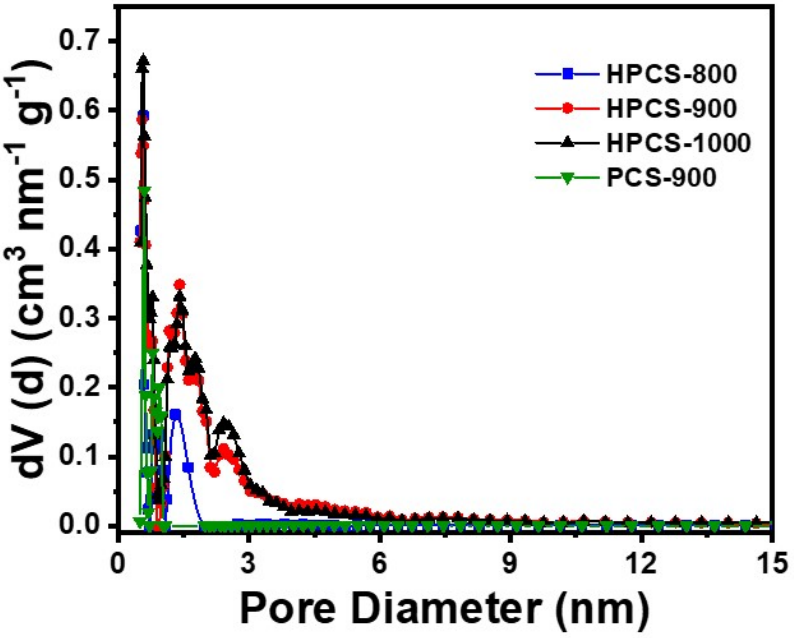

Figure S6. The pore size distributions.

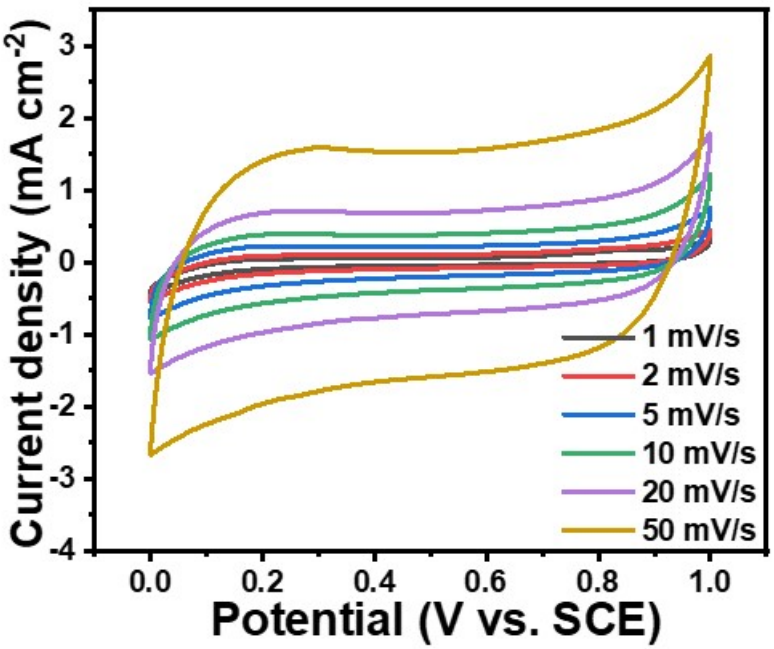

Figure S7. Electrochemical performance measured in a three-electrode system using 2 M $ZnSO_4$ as electrolyte. The CV curves of HPCS-900 at different scan rates.

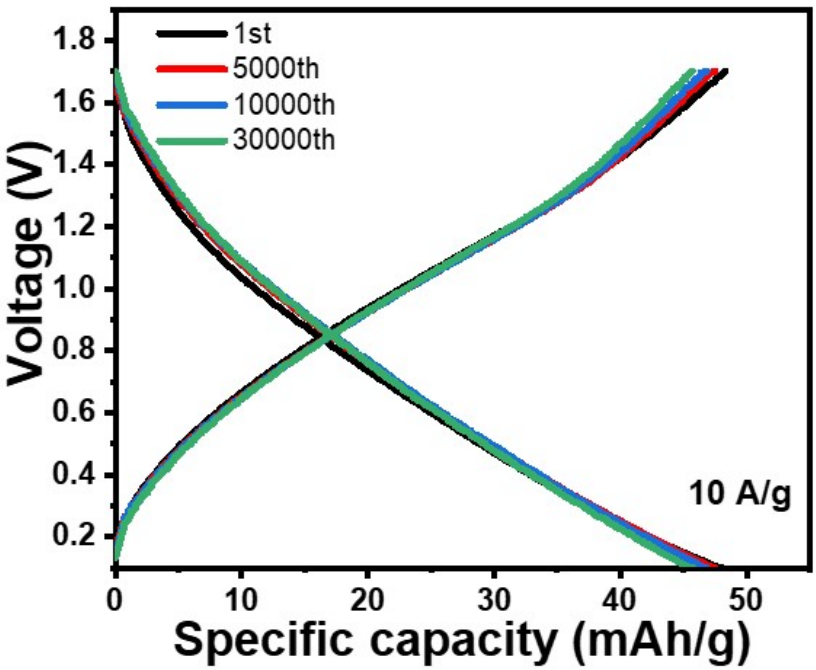

Figure S8. Galvanostatic discharge–charge curves with different cycle numbers at 10 A g^{-1} of HPCS-900-based ZIHCs.

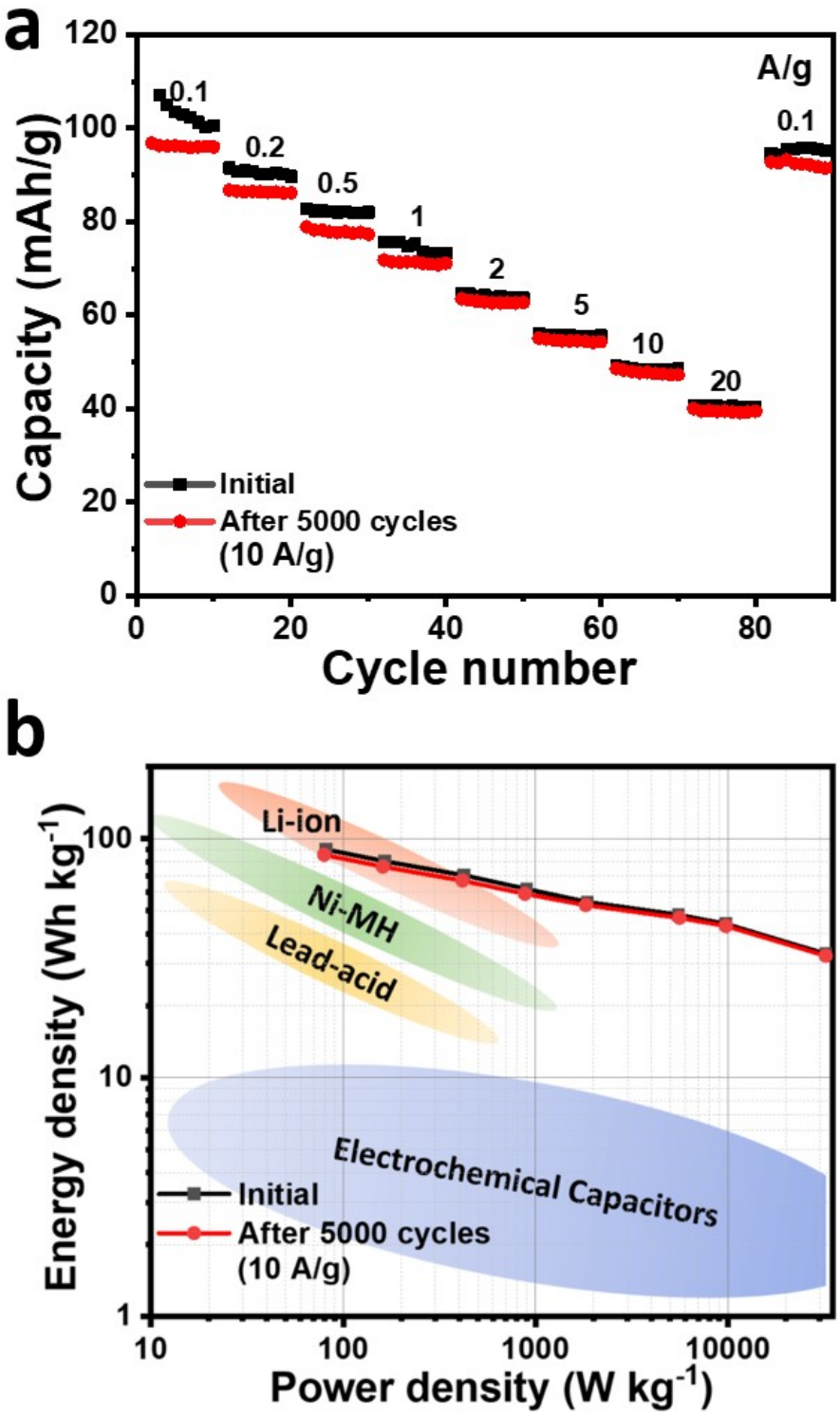

Figure S9. (a) The rate capability and (b) the Ragone plot of HPCS-900-based ZIHCs before and after 5000 cycles at 10A g^{-1}.

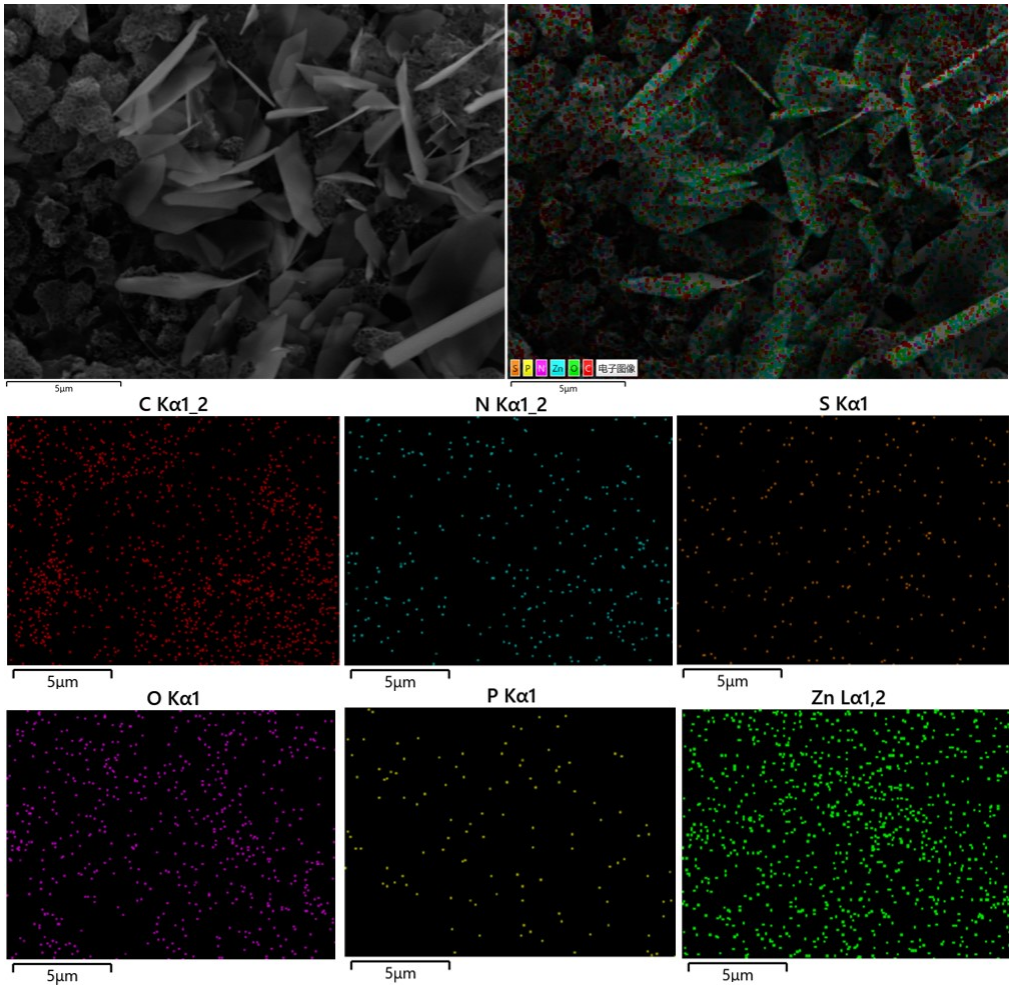

Figure S10. The elementals mapping images of the HPCS-900 cathodes at discharge-0.1V stages.

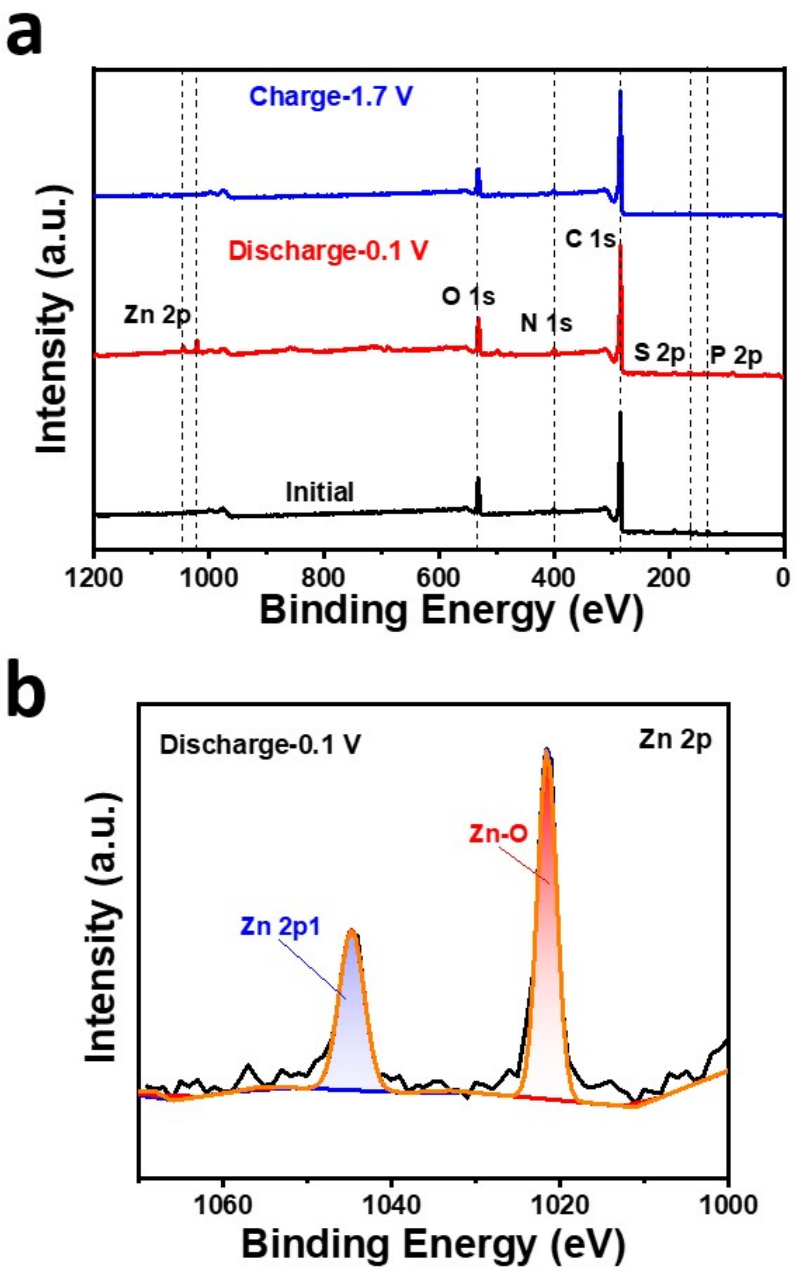

Figure S11. (a) XPS survey spectra of HPCS-900 at the different charging/discharging states and (b) the high-resolution spectra of Zn 2p.

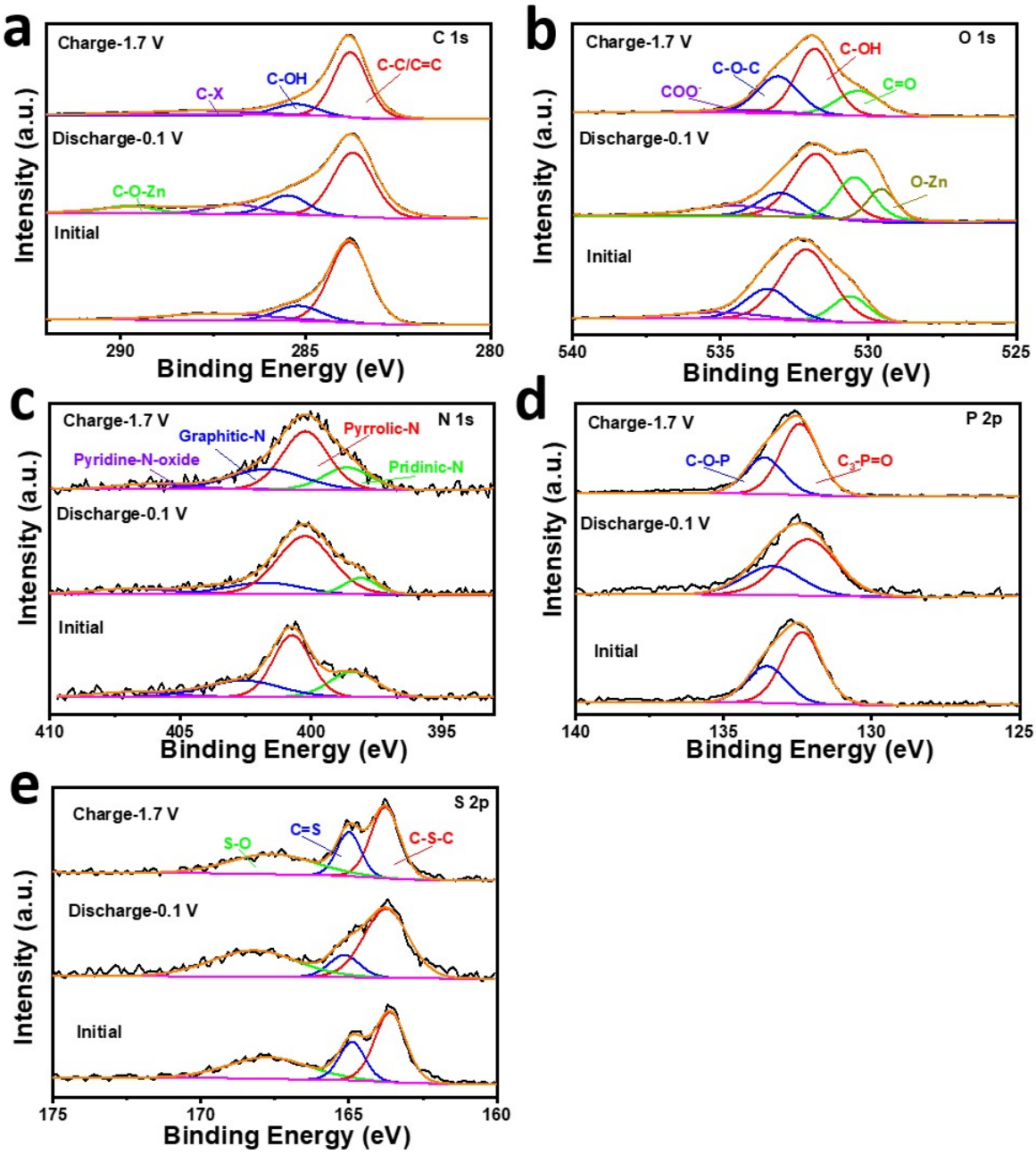

Figure S12. The corresponding XPS high-resolution spectra at the different charging/discharging states of (a) C 1s, (b) O 1s, (c) N 1s, (d) P 2p and (e) S 2p.

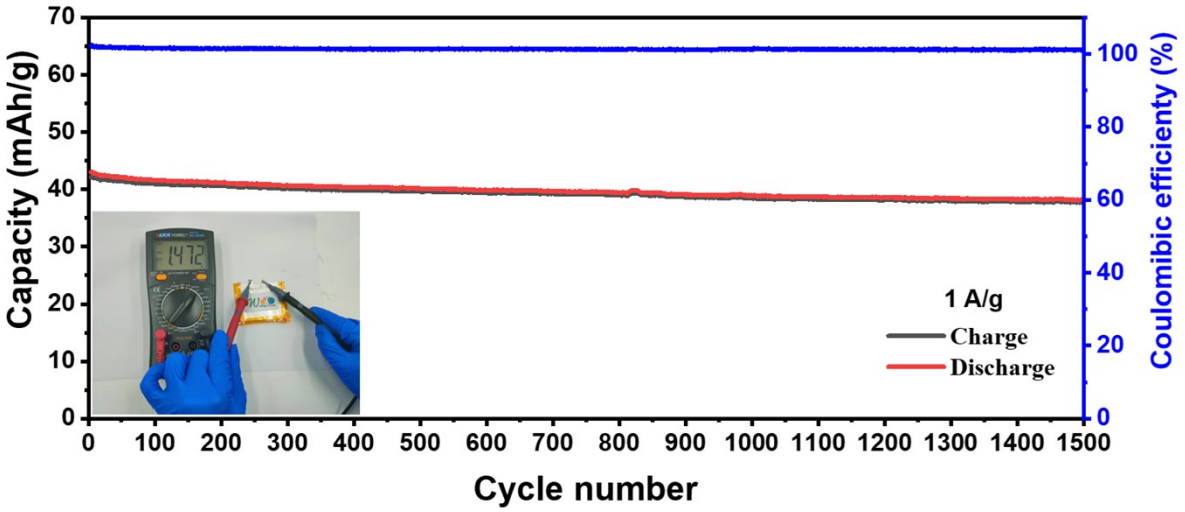

Figure S13. Cycling stability of soft-pack rechargeable ZIHCs device at 1 A g^{-1}.

Supporting Tables

Table S1. BET surface areas and pore volumes of electrode materials.

Sample	S_{BET} [a] ($m^2 g^{-1}$)	V_{total} [b] ($cm^3 g^{-1}$)	V_{micro} [c] ($cm^3 g^{-1}$)	V_{meso} [d] ($cm^3 g^{-1}$)	S_{micro} [c] ($m^2 g^{-1}$)
HPCS-800	**816.03**	**0.672**	**0.246**	**0.426**	**437.74**
HPCS-900	**1176.95**	**0.852**	**0.287**	**0.565**	**877.38**
HPCS-1000	**1249.30**	**0.950**	**0.284**	**0.666**	**862.13**
PCS-900	**391.42**	**0.156**	**0.144**	**0.012**	**360.45**

a The specific surface area were calculated by using multiple BET method.

b The total pore volume were calculated at the relative pressure of 0.99.

c The pore volume and specific surface area of micropores were calculated by using t-plot method.

d The pore volume of mesopores and specific surface area were calculated by subtracting the volume of micropores from the total volume.

Table S2. EDS results of materials (atomic concentration).

Sample	C (%)	N (%)	O (%)	P (%)	S (%)
HPCS-800	**66.69**	**10.98**	**16.12**	**3.81**	**2.40**
HPCS-900	**81.69**	**3.16**	**11.4**	**2.3**	**1.45**
HPCS-1000	**87.32**	**1.17**	**9.68**	**1.18**	**0.65**
PCS-900	**81.31**	**3.37**	**10.9**	**2.88**	**1.54**

Table S3. Summary of various recently reported Zn-based energy storage devices.

Energy storage system	Operating voltage	Capability	Energy density	Cycling stability	Ref.
HPCS//3M $ZnSO_4$//Zn	0.1-1.7 V	253.6 F g^{-1} (0.1 A g^{-1})	90.17 Wh kg^{-1}	95.24% after 30000 cycles	This work
Carbon sheets//2M $Zn(CF_3SO_3)_2$ //Zn	0.2-1.8 V	111 mAh g^{-1} (0.1 A g-1)	109.5 Wh kg^{-1}	92.7% after 50000 cycles	[1]
Oxygen-porous carbon//1M $ZnSO_4$(gelatin)//Zn	0-1.8 V	132.7 mAh g^{-1} (0.2 A g^{-1})	82.36 Wh kg^{-1}	87.6% after 10000 cycles	[2]
PHCA//2M $ZnSO_4$//Zn	0-1.8 V	143.7 mAh g^{-1} (1 A g^{-1})	129.3 Wh kg^{-1}	92% after 10000 cycles	[3]
Corncob-carbon//2M $ZnSO_4$//Zn	0.2-1.8 V	---	94 Wh kg^{-1}	98% after 10000 cycles	[4]
Hollow carbon sphere// hydrogel//Zn	0.15-1.95 V	86.8 mAh g^{-1} (0.5 A g^{-1})	59.7 Wh kg^{-1}	98% after 15000 cycles	[5]
Zn_xMnO_2//2M $ZnSO_4$ +0.4M $MnSO_4$//ACC	0-2 V	145.5 F g^{-1} (2 mA cm^{-2})	---	83.1% after 5000 cycles	[6]
aMEGO//3M $Zn(CF_3SO_3)_2$ //Zn	0-1.9 V	166 F g^{-1} (0.5 A g^{-1})	83.2 Wh kg^{-1}	93% after 80000 cycles	[7]
AC//2M $ZnSO_4$//Zn	0-1.8 V	121 mAh g^{-1} (0.1 A g^{-1})	84 Wh kg^{-1}	91% after 10000 cycles	[8]

AC//2M	0.5-1.5 V	259.4 F g^{-1}	115.4 □Wh	100% after	[9]
$ZnSO_4$//Zn		(0.05 A g^{-1})	cm^{-2}	10000 cycles	
DFs//1M	0.2-1.8 V	246.1 F g^{-1}	70.7	89.9% after	[10]
$ZnSO_4$//Zn		(0.2 A g^{-1})	Wh kg^{-1}	10000 cycles	

Reference

1. Lou, G.; Pei, G.; Wu, Y.; Lu, Y.; Wu, Y.; Zhu, X.; Pang, Y.; Shen, Z.; Wu, Q.; Fu, S.; Chen, H., Combustion conversion of wood to N, O co-doped 2D carbon nanosheets for zinc-ion hybrid supercapacitors. *Chemical Engineering Journal* **2021,** *413*.
2. Zheng, Y.; Zhao, W.; Jia, D.; Liu, Y.; Cui, L.; Wei, D.; Zheng, R.; Liu, J., Porous carbon prepared via combustion and acid treatment as flexible zinc-ion capacitor electrode material. *Chemical Engineering Journal* **2020,** *387*.
3. Fan, H.; Zhou, S.; Chen, Q.; Gao, G.; Ban, Q.; Xu, Z.; He, F.; Hu, G.; Hu, X., Phosphorus in honeycomb-like carbon as a cathode boosting pseudocapacitive properties for Zn-ion storage. *Journal of Power Sources* **2021,** *493*.
4. He, L.; Liu, Y.; Li, C.; Yang, D.; Wang, W.; Yan, W.; Zhou, W.; Wu, Z.; Wang, L.; Huang, Q.; Zhu, Y.; Chen, Y.; Fu, L.; Hou, X.; Wu, Y., A Low-Cost Zn-Based Aqueous Supercapacitor with High Energy Density. *ACS Appl. Energ. Mater.* **2019,** *2* (8), 5835-5842.
5. Chen, S.; Ma, L.; Zhang, K.; Kamruzzaman, M.; Zhi, C.; Zapien, J. A., A flexible solid-state zinc ion hybrid supercapacitor based on co-polymer derived hollow carbon spheres. *Journal of Materials Chemistry A* **2019,** *7* (13), 7784-7790.
6. Chen, Q.; Jin, J.; Kou, Z.; Liao, C.; Liu, Z.; Zhou, L.; Wang, J.; Mai, L., Zn(2+) Pre-Intercalation Stabilizes the Tunnel Structure of MnO2 Nanowires and Enables Zinc-Ion Hybrid Supercapacitor of Battery-Level Energy Density. *Small* **2020,** *16* (14), e2000091.
7. Du, Y.; Chi, X.; Huang, J.; Qiu, Q.; Liu, Y., Long lifespan and high-rate Zn anode boosted by 3D porous structure and conducting network. *Journal of Power Sources* **2020,** *479*.
8. Dong, L.; Ma, X.; Li, Y.; Zhao, L.; Liu, W.; Cheng, J.; Xu, C.; Li, B.; Yang, Q.-H.; Kang, F., Extremely safe, high-rate and ultralong-life zinc-ion hybrid supercapacitors. *Energy Storage Materials* **2018,** *13*, 96-102.
9. Zhang, P.; Li, Y.; Wang, G.; Wang, F.; Yang, S.; Zhu, F.; Zhuang, X.; Schmidt, O. G.; Feng, X., Zn-Ion Hybrid Micro-Supercapacitors with Ultrahigh Areal Energy Density and Long-Term Durability. *Adv Mater* **2019,** *31* (3), e1806005.
10. Jian, Z.; Yang, N.; Vogel, M.; Leith, S.; Schulte, A.; Schönherr, H.; Jiao, T.; Zhang, W.; Müller, J.; Butz, B.; Jiang, X., Flexible Diamond Fibers for High-Energy-Density Zinc-Ion Supercapacitors. *Advanced Energy Materials* **2020,** *10* (44).